

**Asymmetric Framework for Predicting Liquid-Liquid Equilibrium of Ionic
Liquid-Mixed Solvent Systems: II. Prediction of Ternary Systems**

Luke D. Simoni, Alexandre Chapeaux, Joan F. Brennecke and Mark A. Stadtherr*

Department of Chemical and Biomolecular Engineering
University of Notre Dame, Notre Dame, IN 46556, USA

March 2009
(revised, June 2009)

*Author to whom all correspondence should be addressed. Phone (574) 631-9318; Fax (574) 631-8366; Email: markst@nd.edu

Abstract

A new asymmetric framework for modeling liquid-liquid equilibrium (LLE) in electrolyte/mixed-solvent systems is demonstrated, with focus on systems involving a dilute aqueous solution of an ionic liquid (IL). The extent to which this approach is able to *predict* ternary LLE, using parameters obtained from binary and pure component data only, is evaluated. For this purpose, ternary IL/solvent/water systems are used as examples. Comparisons of predicted LLE are made to experimental data representing various types of ternary LLE behavior, as well as to predictions obtained from standard symmetric models. Results indicate that an asymmetric NRTL/eNRTL model provides better predictions of ternary LLE for systems containing ILs and water than standard symmetric models.

Keywords: Liquid-liquid equilibrium; Ionic liquids; Electrolyte models; Extraction; Aqueous systems

1. Introduction

In Part I of this two-part contribution, we introduced an asymmetric framework for modeling liquid-liquid equilibrium (LLE) in electrolyte/mixed-solvent systems. This approach allows for the use of different Gibbs free energy models, representing different degrees of electrolyte dissociation, in different phases. As a first approximation, we focused on the case in which the electrolyte (IL) is either completely dissociated or completely paired (molecular), with the state of the IL depending on the dielectric constant of the mixed solvent and on the concentration of IL in the phase in question. For these assumptions, the applications of interest are systems involving an aqueous phase that is dilute in IL.

In this second part of the contribution, we demonstrate the use of this asymmetric approach in modeling ternary LLE, with focus on systems of the form IL/solvent/water. Of particular interest is the extent to which this approach is able to *predict* ternary LLE, using parameters obtained from binary and pure component data only. To determine this, we will make comparisons of predicted LLE to experimental data representing various types of ternary LLE behavior, as well as to predictions obtained from standard symmetric models. Before presenting these examples, we first discuss the methods used for estimating model parameters and for performing the ternary phase equilibrium calculations.

2. Model Parameters

In this section we outline the general approach used to determine model parameters. Additional problem-specific details, including sources of data, will be provided in Section 4. The models for which parameters are needed are the conventional (symmetric) NRTL, electrolyte-NRTL (eNRTL) and UNIQUAC models and the new asymmetric NRTL/eNRTL model.

2.1 Fully Adjustable Parameters

For each of the models considered, we use only two fully adjustable parameters per binary. For components i and j , these are the binary interaction parameters θ_{ij} and θ_{ji} , as defined in Appendix A (Part I) for NRTL and eNRTL and in Appendix A here for UNIQUAC. The binary interaction parameters θ_{ij} and θ_{ji} will be determined using experimental binary data

only. If data at the exact system temperature are not available, then, unless otherwise noted, the parameters are determined using data at nearby temperatures, and the parameter values at the system temperature are obtained by assuming a linear temperature dependence.

2.1.1 Partially immiscible binaries

For binaries exhibiting a miscibility gap, the model parameters are determined from LLE data (mutual solubility) using the equal chemical potential conditions. For IL/water binaries, the asymmetric NRTL/eNRTL model parameters are determined using the method described in detail in Part I, and the symmetric NRTL, eNRTL, and UNIQUAC parameters are determined using the method given previously by Simoni et al.^{1,2} For IL/solvent and solvent/water binaries, only the symmetric-model parameters are needed (since there are no phases with dissociated IL), and these are obtained using published values (from binary data), if available, or by using the method of Simoni et al.¹

2.1.2 Miscible binaries

It is possible that the IL/solvent and/or solvent/water binaries may be completely miscible. For these cases, only the symmetric-model parameters are needed, and these are determined from either vapor-liquid equilibrium (VLE) or excess enthalpy (h^E) data. If published parameters obtained from VLE data are available then these are used. Otherwise, except for the solvent/water binary in Section 4.1, we use isothermal VLE data and obtain the binary model parameters by globally minimizing the relative least squares objective function $\sum_i (P_i^{\text{exp}} - P_i^{\text{calc}})^2 / P_i^{\text{exp}}$. If no VLE data is available, which is the case only for the IL/solvent binary in Section 4.2, then we obtain the binary model parameters from excess enthalpy data by globally minimizing the relative least square function $\sum_i (h_i^{\text{E,exp}} - h_i^{\text{E,calc}})^2 / h_i^{\text{E,exp}}$. To perform the global optimization we follow Gau et al.³ and use an interval-Newton method. The approach used here differs in that a somewhat more efficient interval-Newton algorithm⁴ is used. By using this approach, we obtain a rigorous guarantee that the relative least squares objective function used has been globally minimized.

2.2 Other Parameter Values

In this section, we discuss the strategies used for setting other model parameters. For the NRTL and eNRTL models, used symmetrically or asymmetrically, the nonrandomness parameter $\alpha_{ij} = \alpha_{ji}$ is not treated as fully adjustable, but rather as fixed at a value that depends on the type of binary data used. If previously published values have been used for the binary interaction parameters, then the accompanying value of α_{ij} is used. Otherwise, we use the conventional values^{5,6} of $\alpha_{ij} = 0.2$ when LLE data are used to obtain the binary interaction parameters, and $\alpha_{ij} = 0.3$ when VLE data are used. For the one case (Section 4.2) of a miscible binary in which h^E data are used, we use the arbitrary high value of $\alpha_{ij} = 0.8$. In our experience, when fitting to h^E data, particularly if endothermic, a relatively large value of α_{ij} is needed to ensure that the resulting parameters lead to a prediction of complete miscibility (convex Gibbs free energy curve). It is well known⁶ that complete miscibility can be forced by using a sufficiently large value of α_{ij} .

For the closest ionic approach parameter ρ in the eNRTL model, we consider values of 5, 8.94, 14.9 and 25, the last three of which also have been used elsewhere.^{1,2,7,8} The effect of increasing ρ is to reduce the importance of the long-range electrostatic contribution in the eNRTL model. As observed previously,^{1,2} when a relatively small value of ρ is used, it may not be possible to find suitable binary parameter values that fit given binary LLE data. Thus, it may be necessary to adjust ρ to a higher value until suitable binary parameters can be found. For symmetric use of the eNRTL model, we use $\rho = 14.9$, as suitable binary parameters can be found using this value for all of the example systems considered here. Although a physical relationship exists^{9,10} between ρ and $\sigma = \sigma_1$, the ionic center-to-center distance used in the asymmetric framework (see Part I, eq 10), this is only roughly approximated here. The default values used here in the asymmetric NRTL/eNRTL model for ρ and σ are $\rho = 5$ and $\sigma = 5 \cdot 10^{-10}$ m. If suitable binary parameter values cannot be found using these ρ and σ values, then we systematically increase ρ and σ , according to the sequence given in Table 1, until suitable binary parameter values can be found for all binaries in the ternary system of interest. The specific values of ρ and σ used in each example are stated in Section 4.

UNIQUAC requires for each pure component i , a “size” (relative volume) parameter r_i and “shape” (relative area) parameter q_i . For the IL species, these parameters were calculated using the Bondi method using IL segment values determined by Nebig et al.¹¹ For the solvent and co-solvent species, these parameters were taken from standard sources.¹²⁻¹⁴ Traditionally, the reference species used in determining the relative area parameter q_i has been the van der Waals $-\text{CH}_2-$ group.¹⁴ However, as explained by Abreu et al.,¹⁵ this choice may make it impossible to find suitable binary parameter values for modeling binary LLE with UNIQUAC, especially when there are components of greatly different sizes and shapes. To alleviate this problem, Abreu et al.¹⁵ suggest using water as an alternative reference species. Following suit, we allow water as an alternative reference species, but use it only when use of $-\text{CH}_2-$ does not permit finding suitable binary parameter values. A coordination number of $Z = 10$ is used for all UNIQUAC calculations.

3. Computation of Phase Equilibrium

For phase equilibrium at constant temperature T and pressure P , the total Gibbs free energy G must be at a global minimum with respect to the number of phases present and their amounts and compositions. To find this global minimum, we use a standard approach^{16,17} in which an equilibrium phase split calculation is used to determine a local minimum of G and then this system is tested for global optimality using phase stability analysis. If necessary, the phase split calculation is then repeated, perhaps changing the number of phases assumed to be present, until a solution is found that meets the global optimality test. The key to this two-stage global optimization procedure for phase equilibrium is the correct solution of the phase stability problem, itself a global minimization problem. To ensure correct solution of the phase stability problem, we extend the approach of Tessier et al.¹⁸ This method is based on tangent plane analysis^{16,19,20} and uses a rigorous global minimization technique based on an interval-Newton approach, thus providing a mathematical and computational guarantee^{21,22} of global optimality. Tessier et al.¹⁸ considered only the case of a symmetric model with no dissociation. For the computations reported here, we have extended this approach to the new case of an asymmetric model with dissociation, using the objective functions derived in Part I. The approach used here also differs from that of Tessier et al.¹⁸ in that a somewhat more efficient interval-Newton algorithm⁴ is used.

4. Examples

In this section, we give four examples that demonstrate the use of the asymmetric framework for modeling LLE in electrolyte/mixed-solvent systems, in particular ternary IL (1)/alcohol (2)/water (3) systems. For each example, we discuss how the model parameters were obtained from binary data, and then we use these parameters to predict the ternary LLE. For the asymmetric framework we use NRTL for a molecular phase and eNRTL for a dissociated phase, as described in Part 1. Predictions from the asymmetric NRTL/eNRTL model are compared to experimental data, and to predictions based on the conventional (symmetric) NRTL, eNRTL, and UNIQUAC models. The example systems are listed in Table 2, which also indicates the type⁵ of ternary LLE observed experimentally for each system, and provides a key to the Figures in which the predictions (ternary diagrams) for each system can be found. Generic depictions of the different types of ternary phase behavior referred to in Table 2, and in the discussion below, as shown in Figure 1. All examples are at conditions of atmospheric pressure. The cut-off values (explained in Part I) used in the asymmetric modeling framework are $\epsilon_c = 40$ and $x_c = 0.10$.

The binary interaction parameters used in each example are compiled in Tables 3-5 for the symmetric NRTL, UNIQUAC and eNRTL models, respectively, and in Table 6 for the asymmetric NRTL/eNRTL model. Pure component properties used are tabulated in Table 7, which gives data for properties needed in the electrostatic term of the eNRTL model, namely molecular weight (M_i), density (d_i) and dielectric constant (ϵ_i), and in Table 8, which gives data for the UNIQUAC size (r_i) and shape (q_i) parameters.

4.1 Example 1: [hmim][Tf₂N]/Ethanol/Water at 295 K

This example involves the ternary system of 1-hexyl-3-methylimidazolium bis(trifluoromethylsulfonyl)imide ([hmim][Tf₂N]) (component 1), ethanol (EtOH) (component 2), and water (component 3) at $T = 295$ K. This system exhibits Type 1 ternary LLE behavior experimentally.²³ As shown in Figure 1, a Type 1 system exhibits a single phase envelope emanating from a single binary miscibility gap, which in this case corresponds to the [hmim][Tf₂N]/water binary. LLE data for [hmim][Tf₂N]/water are given by Chapeaux et al.²⁴ and these data were used to estimate the model parameters for this binary. The other two

binaries, [hmim][Tf₂N]/EtOH and EtOH/water, are totally miscible at the system temperature. Unfortunately, VLE data for IL/EtOH was not available at the temperature of the system. Therefore, VLE data measured by Kato and Gmehling²⁵ at 353.16 K were used to estimate the model parameters for this binary. For the EtOH/water binary, we used NRTL parameters from Kurihara et al.,²⁶ including $\alpha_{23} = 0.1448$. The UNIQUAC parameters for the EtOH/water binary were estimated using data at 295.75 K from Gmehling et al.²⁷ by fitting directly to the equifugacity conditions for VLE. For the asymmetric model predictions, the closest ionic approach parameter values used in this example are $\rho = 5$ and $\sigma = 1 \cdot 10^{-9}$ m. In order to calculate the IL reference energy, the asymmetric model requires a value for the IL's static dielectric constant (see Part I). Dielectric constants have been measured²⁸ for a series of 1-alkyl-3-methylimidazolium bis(trifluoromethylsulfonyl)imide ILs. Extrapolating these values with respect to alkyl chain length yields a dielectric constant estimate for [hmim][Tf₂N] of $\epsilon_1 = 11.4$. For the symmetric use of UNIQUAC, the reference species used for the pure component shape parameters is the $-\text{CH}_2-$ group.

For the symmetric NRTL, UNIQUAC, and eNRTL models, the predicted ternary behavior is shown in Figure 2. It can be seen that UNIQUAC provides a remarkably good prediction of the two-phase envelope and plait point, though the tie line slopes are somewhat steeper than those measured experimentally. NRTL provides a somewhat better slope for the tie lines than UNIQUAC, but with greater overestimation of the two-phase envelope. Overall, UNIQUAC is the best of the symmetric models in predicting the ternary LLE for this system.

Figure 3 shows the prediction from the asymmetric NRTL/eNRTL model, with comparison to the UNIQUAC prediction, the best of the symmetric models for this system. A close qualitative inspection of Figure 2 indicates that the asymmetric NRTL/eNRTL prediction is somewhat better than the UNIQUAC prediction, in terms of both the two-phase envelope size and the slope of the tie lines. To obtain a more quantitative comparison, for each experimental tie line, we took the midpoint and used it as the feed composition to calculate phase equilibrium (endpoints of a calculated tie line). These calculated values were then compared to the experimental endpoints of the tie line, and the average absolute deviation

$$\text{AAD} = \frac{1}{N} \sum_{k=1}^{TL} \sum_{j=1}^2 \sum_{i=1}^3 \left| x_{i,k,\text{exp}}^{(j)} - x_{i,k,\text{calc}}^{(j)} \right| \quad (1)$$

was determined. Here $x_{i,k,\text{calc}}^{(j)}$ is the calculated mole fraction of component i in phase j based on the midpoint of tie line k , and $x_{i,k,\text{exp}}^{(j)}$ is the corresponding experimental value. $TL = 12$ is the number of tie lines used for the comparison, and $N = (2)(3)(TL)$ is the number of terms in the summation. For the UNIQUAC prediction, $AAD = 0.0311$, and for the asymmetric NRTL/eNRTL prediction, $AAD = 0.0202$. Two experimental tie lines very close to the plait point were not used in this comparison, since UNIQUAC slightly overshoots the plait point, and asymmetric NRTL/eNRTL slightly undershoots it. For this example, the UNIQUAC model provides a remarkably good prediction of the ternary phase behavior. The new asymmetric framework, using NRTL and eNRTL, provides a remarkably good prediction as well, one that is even somewhat better than the UNIQUAC prediction.

4.2 Example 2: [HOhmim][Tf₂N]/1-Butanol/Water at 295 K

For this example, we consider the ternary system of 1-hydroxyhexyl-3-methylimidazolium bis(trifluoromethylsulfonyl)imide ([HOhmim][Tf₂N]) (component 1), 1-butanol (BuOH) (component 2), and water (component 3) at $T = 295$ K. This system exhibits a Type 2 ternary LLE system experimentally.²⁹ A Type 2 system exhibits a phase envelope that spans the composition space and connects two binary miscibility gaps, as shown generically in Figure 1. In this example, the immiscible binaries are [HOhmim][Tf₂N]/water and BuOH/water. LLE data for [HOhmim][Tf₂N]/water are given by Chapeaux et al.³⁰ and these data were used to estimate the interaction parameters for this binary. For the BuOH/water binary, LLE data from Sørensen and Arlt⁵ were used for the parameter estimation. The third binary, [HOhmim][Tf₂N]/BuOH is completely miscible at the system temperature. Since no VLE data is available for this binary, we used h^E data,³¹ which is available for 40 °C, to estimate the model parameters. The NRTL parameters found for [HOhmim][Tf₂N]/BuOH (with $\alpha_{12} = 0.8$) yield a miscible binary system. However, for UNIQUAC and eNRTL, the model parameters found for this binary yield only a partially miscible system. Thus, for symmetric model predictions we focus on NRTL only. For the asymmetric model predictions, the closest ionic approach parameter values used in this example are $\rho = 8.94$ and $\sigma = 5 \cdot 10^{-9}$ m. No experimental value of the dielectric constant for [HOhmim][Tf₂N] is available. We took this value to be $\epsilon_1 = 15$. This is based on the estimated dielectric constant (11.4) of [hmim][Tf₂N], from the previous example, and assuming that addition of a hydroxyl group may somewhat increase the dielectric constant.

The symmetric NRTL prediction is shown in Figure 4. This predicts a three-phase region, with an additional two-phase envelope, terminating in a plait point, that emanates from the IL/BuOH side of the three-phase region. This prediction is qualitatively incorrect, as neither of these features is observed experimentally.

Figure 5 shows the asymmetric NRTL/eNRTL prediction for this system. This prediction of Type 2 ternary behavior is in qualitative agreement with the experimental measurements, and there is good quantitative accuracy as well. Note that for the IL/BuOH and BuOH/water binaries the model parameters are the same in the symmetric NRTL model as in the asymmetric NRTL/eNRTL model. The parameters in the IL/water binary are different in the asymmetric NRTL/eNRTL model in order to account for the dissociation of IL in the dilute aqueous phase. By using an asymmetric model that allows for dissociation of IL in a dilute aqueous phase, but not in other phases, we have been able to obtain a significantly improved prediction of the ternary behavior in this example system.

4.3 Example 3: [bmim][PF₆]/Ethanol/Water at 290, 298 and 313 K

The example focuses on the ternary system of 1-butyl-3-methylimidazolium hexafluorophosphate ([bmim][PF₆]) (component 1), ethanol (component 2) and water (component 3) at $T = 290$ K, $T = 298$ K, and $T = 313$ K. Experimentally, this system exhibits Type 2a ternary LLE diagrams.³² In Type 2a ternary diagrams, there are two distinct phase envelopes corresponding to two binary miscibility gaps, and complete miscibility at intermediate compositions (see Figure 1). As noted in a previous study,² these types of ternary LLE systems are difficult to predict with g^E models fit to binary data. It may be difficult to obtain even a proper qualitative prediction (i.e., Type 2a rather than Type 2). LLE data for [bmim][PF₆]/water are available from Najdanovic-Visak et al.³³ and Anthony et al.,³⁴ and these data were used to estimate the interaction parameters for this binary. For the [bmim][PF₆]/EtOH binary, experimental data from Najdanovic-Visak et al.³² were used to estimate the binary parameters. For neither of these binaries was it possible to obtain UNIQUAC parameters to represent the miscibility gaps. This is a well-known issue¹⁵ with UNIQUAC, which might be addressed by considering an even larger reference species for the pure component shape parameters (we considered only $-\text{CH}_2-$ and water). Thus, symmetric predictions were made using only NRTL and eNRTL. For the miscible EtOH/water binary, we used NRTL parameters from Kurihara et al.,²⁶ including $\alpha_{23} = 0.1448$. For the asymmetric model predictions, the closest ionic approach

parameter values used in this example are $\rho = 8.94$ and $\sigma = 5 \cdot 10^{-9}$ m. The dielectric constant for [bmim][PF₆] was measured by Weingärtner³⁵ as $\epsilon_1 = 11.4$.

We have considered the application of the symmetric NRTL and eNRTL models to this system in a previous study.² Figure 6 shows these symmetric-model predictions for the 298 K case, together with the experimental data. Note that experimental tie lines are not available, just cloud point measurements to obtain an approximate binodal curve. Also note that there are small discrepancies between the experimental and calculated binary miscibility gaps. This is due solely to an inconsistency between the experimental binary data used to perform the predictions and the experimental ternary data used for comparison. Both NRTL and eNRTL, applied symmetrically, predict Type 2 LLE behavior, not Type 2a, as observed experimentally.

Figure 7 shows the asymmetric NRTL/eNRTL prediction at 298 K. Here we see a dramatic qualitative improvement in the prediction. We now see Type 2a behavior predicted on the aqueous side of the diagram, with this two-phase envelope terminating in a plait point. However, on the alcohol side of the diagram, the two-phase envelope is still of Type 2 character, as it does not terminate in a plait point. Instead this two-phase envelope will terminate when the mixed solvent dielectric constant in the IL-lean phase ($x_1 < x_c = 0.10$) reaches the $\epsilon_c = 40$ cut-off for a molecular phase model. This type of discontinuity must be recognized as a possibility when an asymmetric model for LLE is used. It is interesting to note that if the cut-off on the mixed solvent dielectric constant is relaxed, so that the IL is considered dissociated in dilute solution ($x_1 < x_c$) with any mixture of water and ethanol, then the prediction of the asymmetric NRTL/eNRTL model becomes completely Type 2a (i.e., both two-phase envelopes terminate in a plait point).

For the 290 K case, both the symmetric NRTL and eNRTL models again predict Type 2 LLE behavior,² not Type 2a, as indicated by cloud point measurements. Figure 8 shows the cloud point data, along with the prediction from the asymmetric NRTL/eNRTL model at 290 K. The situation is very similar to that observed for the 298 K case. The asymmetric-model prediction captures the two-phase envelope on the aqueous side of the diagram, but not on the alcohol side. Finally for the 313 K case, which experimentally is Type 2a, the symmetric NRTL model again predicts² Type 2 behavior, but the symmetric eNRTL model correctly predicts² Type 2a. Figure 9 shows that the asymmetric NRTL/eNRTL model also correctly predicts Type

2a. The symmetric eNRTL prediction significantly overestimates² the size of the two-phase envelope on the aqueous side, and the asymmetric-model prediction significantly overestimates the size of the two-phase envelope on the alcohol side.

4.4 Example 4: [bmim][Tf₂N]/1-Butanol/Water at 288 K

This example involves the ternary system of 1-butyl-3-methylimidazolium bis(trifluoromethylsulfonyl)imide ([bmim][Tf₂N]) (component 1), 1-butanol (component 2), and water (component 3) at $T = 288$ K. For this system, all three binary subsystems have a miscibility gap. As shown in Figure 1, there are multiple types of possible ternary behavior for the case of three binary miscibility gaps,⁵ of which Types 3a and 3b are of interest here. A Type 3b system has three distinct two-phase envelopes, each emanating from one of the binary miscibility gaps and terminating in a plait point. In a Type 3a system, two of these three envelopes merge into one, i.e., there is one two-phase envelope that connects two of the binary miscibility gaps and another two-phase envelope that emanates from the remaining binary miscibility gap and terminates in a plait point. Najdanovic-Visak et al.³⁶ have presented limited cloud point data for this system, interpolated to 288 K. This is consistent with either Type 3a or 3b behavior, though Najdanovic-Visak et al.³⁶ proposed the approximate Type 3b diagram shown for reference in Figure 10. However, recent experiments by Morton and Davis³⁷ imply, at least qualitatively (we do not believe that their measurements are quantitatively correct, as discussed in Appendix B), that there is a much larger two-phase region extending roughly between the BuOH/water and [bmim][Tf₂N]/water miscibility gaps, even at the higher temperature of 298 K. This suggests that this system is actually Type 3a, with one two-phase region connecting the BuOH/water and [bmim][Tf₂N]/water miscibility gaps, and another emanating from the [bmim][Tf₂N]/butanol miscibility gap and going to a plait point. Davis and Morton³⁷ also state that they observed a three-phase equilibrium state for this system, but we believe that this is likely to be spurious, as discussed in Appendix B.

For the [bmim][Tf₂N]/water binary, model parameters were determined from the LLE data of Crosthwaite et al.,³⁸ for the [bmim][Tf₂N]/BuOH binary from the data of Najdanovic-Visak et al.,³⁶ and for the BuOH/water binary from data given by Sørensen and Arlt.⁵ For the asymmetric model predictions, the closest ionic approach parameter values used in this example are $\rho = 5$ and $\sigma = 1 \cdot 10^{-9}$ m. The dielectric constant of [bmim][Tf₂N] was measured by Daguenet

et al.²⁸ as $\epsilon_1 = 11.5$. For the symmetric use of UNIQUAC the reference species for the pure component shape parameters is water.

As can be seen from Figures 10 and 11, the symmetric-model predictions² using NRTL and UNIQUAC, respectively, yield qualitatively incorrect Type 3 ternary systems. Type 3 systems are characterized by the presence of three two-phase envelopes that emanate from their respective binary miscibility gaps and then converge in a three-phase region, as shown in Figure 1. The size of three-phase region predicted by UNIQUAC, and hence the overall immiscibility of the system, is somewhat smaller than that predicted by NRTL. The symmetric eNRTL prediction² is shown in Figure 12 and has the Type 3a behavior that we believe to be qualitatively correct, as explained above. This is a significant improvement over the NRTL and UNIQUAC predictions, but still deviates considerably from the experimental cloud point observation at $x_2 \approx 0.23$ (BuOH).

Figure 13 compares the asymmetric NRTL/eNRTL model prediction to the symmetric eNRTL model prediction and the experimental cloud points. The asymmetric NRTL/eNRTL model also predicts a Type 3a system. Although there is not a dramatic change compared to the symmetric eNRTL prediction, the asymmetric NRTL/eNRTL prediction does better capture the cloud point observation at $x_2 \approx 0.23$ (BuOH), improving the shape of the binodal curve for the two-phase region involving a dilute aqueous phase. The improved predictions provided by the asymmetric NRTL/eNRTL model and the symmetric eNRTL model on this problem, and on the previous one, indicate the importance of accounting for electrostatic forces in problems involving dilute aqueous solutions of ILs.

5. Concluding Remarks

In the examples above, we have used the asymmetric framework presented in Part I of this contribution to predict ternary LLE, using parameters obtained from binary and pure component data only. Comparisons of the predicted LLE were made to experimental data representing various types of ternary LLE behavior, as well as to predictions obtained from standard symmetric models. This is a stringent test of the suitability of various models for describing LLE in systems containing ILs and water. We have found that, for systems of the type considered here, namely systems involving an aqueous phase dilute in IL, an asymmetric

NRTL/eNRTL model provides better predictions than standard symmetric models (NRTL, UNIQUAC, eNRTL). Examples 3 and 4, involving Type 2a and 3a ternary behavior, respectively, suggest the importance of including an electrostatic contribution in the Gibbs free energy for systems involving dilute aqueous solutions of ILs. Doing this asymmetrically, so that IL dissociation is allowed only in the aqueous phase, provides improvements over the symmetric electrolyte model (eNRTL) in all examples. In future work, we will consider partial dissociation and application to nonaqueous systems.

Acknowledgements

This work was supported in part by the Department of Energy under Grant DE-FG36-08GO88020. Additional support was provided by a University of Notre Dame Arthur J. Schmitt Presidential Fellowship (LDS).

Literature Cited

- (1) Simoni, L. D.; Lin, Y.; Brennecke, J. F.; Stadtherr, M. A. Reliable computation of binary parameters in activity coefficient models for liquid-liquid equilibrium. *Fluid Phase Equilib.* **2007**, *255*, 138-146.
- (2) Simoni, L. D.; Lin, Y.; Brennecke, J. F.; Stadtherr, M. A. Modeling liquid-liquid equilibrium of ionic liquid systems with NRTL, electrolyte-NRTL, and UNIQUAC. *Ind. Eng. Chem. Res.* **2008**, *47*, 256-272.
- (3) Gau, C.-Y.; Brennecke, J. F.; Stadtherr, M. A. Reliable nonlinear parameter estimation in VLE modeling. *Fluid Phase Equilib.* **2000**, *168*, 1-18.
- (4) Lin, Y.; Stadtherr, M. A. LP Strategy for Interval-Newton Method in Deterministic Global Optimization. *Ind. Eng. Chem. Res.* **2004**, *43*, 3741-3749.
- (5) Sørensen, J. M.; Arlt, W. *Liquid-Liquid Equilibrium Data Collection*; DECHEMA: Frankfurt/Main, Germany, 1979-1980.
- (6) Renon, H.; Prausnitz, J. M. Local compositions in thermodynamic excess functions for liquid mixtures. *AIChE J.* **1968**, *14*, 135-144.
- (7) Pitzer, K. S. Electrolytes. From dilute solutions to fused salts. *J. Amer. Chem. Soc.* **1980**, *102*, 2902-2906.
- (8) Chen, C.-C.; Britt, H. I.; Boston, J. F.; Evans, L. B. Local composition model for excess Gibbs energy of electrolyte solutions, Part I: Single solvent, single completely dissociated electrolyte systems. *AIChE J.* **1982**, *28*, 588-596.
- (9) Pitzer, K. S. Electrolyte theory-improvements since Debye and Hückel. *Accounts of Chemical Research* **1977**, *10*, 371-377.
- (10) Pitzer, K. S.; Li, Y. -. Thermodynamics of aqueous sodium chloride to 823 K and 1 kilobar (100 MPa). *Proc. Natl. Acad. Sci. USA* **1983**, *80*, 7689-7693.
- (11) Nebig, S.; Bölts, R.; Gmehling, J. Measurement of vapor-liquid equilibria (VLE) and excess enthalpies (H^E) of binary systems with 1-alkyl-3-methylimidazolium

bis(trifluoromethylsulfonyl)imide and prediction of these properties and γ^∞ using modified UNIFAC (Dortmund). *Fluid Phase Equilib.* **2007**, *258*, 168-178.

(12) Smith, J. M.; Van Ness, H. C.; Abbott, M. M. *Introduction to Chemical Engineering Thermodynamics*; McGraw-Hill: New York, NY, 2001.

(13) Anderson, T. F.; Prausnitz, J. M. Application of the UNIQUAC equation to calculation of multicomponent phase equilibria. 1. Vapor-liquid equilibria. *Ind. Eng. Chem. Process Des. Dev.* **1978**, *17*, 552-561.

(14) Abrams, D. S.; Prausnitz, J. M. Statistical thermodynamics of liquid mixtures: A new expression for the excess Gibbs energy of partly or completely miscible systems. *AIChE J.* **1975**, *21*, 116-128.

(15) Abreu, C. R. A.; Castier, M.; Tavares, F. W. A phase stability analysis of the combinatorial term of the UNIQUAC model. *Chem. Eng. Sci.* **1999**, *54*, 893-896.

(16) Michelsen, M. L. The isothermal flash problem. Part I: Stability. *Fluid Phase Equilib.* **1982**, *9*, 1-19.

(17) Michelsen, M. L. The isothermal flash problem. Part II: Phase-split calculation. *Fluid Phase Equilibria* **1982**, *9*, 21-40.

(18) Tessier, S. R.; Brennecke, J. F.; Stadtherr, M. A. Reliable phase stability analysis for excess Gibbs energy models. *Chem. Eng. Sci.* **2000**, *55*, 1785-1796.

(19) Baker, L. E.; Pierce, A. C.; Luks, K. D. Gibbs energy analysis of phase equilibria. *Soc. Petrol. Engrs. J.* **1982**, *22*, 731-742.

(20) Prausnitz, J. M.; Lichtenthaler, R. N.; Gomes de Azevedo, E. *Molecular Thermodynamics of Fluid-Phase Equilibria*; Prentice Hall: Upper-Saddle River, New Jersey, 1999.

(21) Neumaier, A. *Interval Methods for Systems of Equations*; Cambridge University Press: Cambridge, UK, 1990.

(22) Kearfott, R. B. *Rigorous Global Search: Continuous Problems*; Kluwer Academic Publishers: Dordrecht, The Netherlands, 1996.

(23) Chapeaux, A.; Simoni, L. D.; Ronan, T.; Stadtherr, M. A.; Brennecke, J. F. Extraction of alcohols from water with 1-hexyl-3-methylimidazolium bis(trifluoromethylsulfonyl)imide. *Green Chem.* **2008**, *10*, 1301-1306.

(24) Chapeaux, A.; Simoni, L. D.; Stadtherr, M. A.; Brennecke, J. F. Liquid phase behavior of ionic liquids with water and 1-octanol and modeling of 1-octanol/water partition coefficients. *J. Chem. Eng. Data* **2007**, *52*, 2462-2467.

(25) Kato, R.; Gmehling, J. Systems with ionic liquids: Measurement of VLE and gamma(infinity) data and prediction of their thermodynamic behavior using original UNIFAC, mod. UNIFAC(Do) and COSMO-RS(O1). *J. Chem. Thermodyn.* **2005**, *37*, 603-619.

(26) Kurihara, K.; Nakamichi, M.; Kojima, K. Isobaric Vapor-Liquid Equilibria for Methanol + Ethanol + Water and the Three Constituent Binary Systems. *J. Chem. Eng. Data* **1993**, *38*, 446-449.

(27) Gmehling, J.; Onken, U.; Arlt, W. *Vapor-liquid Equilibrium Data Collection, Chemistry Data Series, Vol. I, Parts 1-8*; DECHEMA: Frankfurt/Main, Germany, 1977-1990.

(28) Daguinet, C.; Dyson, P. J.; Krossing, I.; Oleinikova, A.; Slattery, J.; Wakai, C.; Weingartner, H. Dielectric response of imidazolium-based room-temperature ionic liquids. *J. Phys. Chem. B* **2006**, *110*, 12682-12688.

(29) Chapeaux, A.; Ronan, T.; Simoni, L. D.; Brennecke, J. F.; Stadtherr, M. A. Separation of water and alcohols using 1-(6-hydroxyhexyl)-3-methylimidazolium bis(trifluoromethylsulfonyl)imide and 1-hexyl-3-methylimidazolium tris(pentafluoroethyl)trifluorophosphate. **2009**, Manuscript in preparation.

(30) Chapeaux, A.; Andrews, N.; Brennecke, J. F. Liquid-Liquid behavior of ILs in water and 1-hexanol. *J. Chem. Eng. Data* **2009**, Manuscript in preparation.

(31) Chapeaux, A.; Brennecke, J. F. Excess enthalpies and enthalpies of vaporization for various ionic liquid-alcohol mixtures. **2009**, Manuscript in preparation.

(32) Najdanovic-Visak, V.; Esperança, J. M. S. S.; Rebelo, L. P. N.; da Ponte, M. N.; Guedes, H. J. R.; Seddon, K. R.; de Sousa, H. C.; Szydłowski, J. Pressure, Isotope, and Water Co-solvent Effects in Liquid-Liquid Equilibria of (Ionic Liquid + Alcohol) Systems. *J. Phys. Chem. B* **2003**, *107*, 12797-12807.

(33) Najdanovic-Visak, V.; Esperança, J. M. S. S.; Rebelo, L. P. N.; da Ponte, M. N.; Guedes, H. J. R.; Seddon, K. R.; Szydłowski, J. Phase behaviour of room temperature ionic liquid solutions: an unusually large co-solvent effect in (water + ethanol). *Phys. Chem. Chem. Phys.* **2002**, *4*, 1701-1703.

(34) Anthony, J. L.; Maginn, E. J.; Brennecke, J. F. Solution thermodynamics of imidazolium-based ionic liquids and water. *J. Phys. Chem. B* **2001**, *105*, 10942-10949.

(35) Weingärtner, H. The static dielectric constant of ionic liquids. *Z. Phys. Chem.* **2006**, *220*, 1395-1405.

(36) Najdanovic-Visak, V.; Rebelo, L. P. N.; da Ponte, M. N. Liquid-liquid behaviour of ionic liquid-1-butanol-water and high pressure CO₂-induced phase changes. *Green Chem.* **2005**, *7*, 443-450.

(37) Davis, S. E.; Morton III, S. A. Investigation of ionic liquids for the separation of butanol and water. *Sep. Sci. Technol.* **2008**, *43*, 2460-2472.

(38) Crosthwaite, J. M.; Aki, S. N. V. K.; Maginn, E. J.; Brennecke, J. F. Liquid Phase Behavior of Imidazolium-Based Ionic Liquids with Alcohols. *J. Phys. Chem. B* **2004**, *108*, 5113-5119.

(39) Smyth, C. P.; Stoops, W. N. The Dielectric Polarization of Liquids. VI. Ethyl Iodide, Ethanol, Normal-Butanol and Normal-Octanol. *J. Am. Chem. Soc.* **1929**, *51*, 3312-3329.

(40) Fernández, D. P.; Goodwin, A. R. H.; Lemmon, E. W.; Levelt Sengers, J. M. H.; Williams, R. C. A formulation for the static permittivity of water and steam at temperatures from 238 K to 873 K at pressures up to 1200 MPa, including derivatives and Debye-Hückel coefficients. *J. Phys. Chem. Ref. Data* **1997**, *26*, 1125-1166.

Appendix A

For the UNIQUAC model,¹⁴

$$\frac{g^E}{RT} = \frac{g_{\text{comb}}}{RT} + \frac{g_{\text{res}}}{RT}, \quad (\text{A1})$$

$$\frac{g_{\text{comb}}}{RT} = \sum_{i=1}^n x_i \ln \frac{\Phi_i}{x_i} + 5 \sum_{i=1}^n q_i x_i \ln \frac{\theta_i}{\Phi_i}, \quad (\text{A2})$$

$$\frac{g_{\text{res}}}{RT} = - \sum_{i=1}^n q_i x_i \ln \left(\sum_{j=1}^n \theta_j \tau_{ji} \right), \quad (\text{A3})$$

$$\Phi_i = \frac{r_i x_i}{\sum_{j=1}^n r_j x_j}, \quad (\text{A4})$$

$$\theta_i = \frac{q_i x_i}{\sum_{j=1}^n q_j x_j} \quad (\text{A5})$$

and

$$\tau_{ij} = \exp \left(\frac{-\Delta u_{ij}}{RT} \right). \quad (\text{A6})$$

Here, r_i and q_i represent a relative volume (size) and surface area (shape), respectively, for component i . It follows that Φ_i and θ_i are volume and surface area fractions, respectively, for component i . The binary interaction parameters $\theta_{ij} = \Delta u_{ij}$ are estimated from experimental binary data.

Appendix B

Davis and Morton³⁷ have recently reported experimental measurements (two-phase tie lines) of LLE in the ternary systems [bmim][Tf₂N]/1-butanol/water (Example 4) and [hmim][Tf₂N]/1-butanol/water at 298 K. Based on our own measurements²³ of LLE in the latter system, we do not believe that the results of Davis and Morton³⁷ are quantitatively correct for either system.

Figure B1 shows the results of our measurements²³ of tie lines in the two-phase region for [hmim][Tf₂N]/1-butanol/water at 295 K. Each tie line was based on three replicates of the feed composition. The estimated uncertainty in the equilibrium compositions was ± 3 mol%. The weight fraction of each component was measured independently, and these summed to one within 5 mol%. Figure B1 also shows the measurements of Davis and Morton³⁷ for this same system at 298 K. There is clearly a large quantitative discrepancy between the two sets of data. Davis and Morton³⁷ did not use replicate feed compositions and did not estimate the uncertainty in their equilibrium composition measurements. They measured the weight fractions of only two of the components, [hmim][Tf₂N] and 1-butanol, and calculated the water composition to make the weight fractions sum to one. Because they did not measure the water composition independently, there was no check on likely errors in the measurements of the other two components. Potential sources for these errors will be discussed elsewhere. Because their measurements for the [hmim][Tf₂N]/1-butanol/water system are quantitatively incorrect, we do not believe that their measurements for the [bmim][Tf₂N]/1-butanol/water system are quantitatively correct either.

For both of the ternary systems [bmim][Tf₂N]/1-butanol/water and [hmim][Tf₂N]/1-butanol/water at 298 K, Davis and Morton³⁷ have reported observing a three-phase equilibrium state while exploring the two-phase region. They do not give the exact feed composition at which this was seen, nor the compositions of the three phases. In our study²³ of the [hmim][Tf₂N]/1-butanol/water system at 295 K, we did not observe any three-phase equilibrium states. The “three-phase” observation of Davis and Morton³⁷ is likely due to the occurrence of a phase density inversion that occurs as the fraction of 1-butanol increases. At low 1-butanol fraction, the aqueous phase is the less dense of the two equilibrium phases. As the fraction of 1-butanol is increased in the two-phase region, eventually the aqueous phase becomes the denser of the two equilibrium phases. Thus, at some point in the two-phase region, the density of the two

phases is the same. When at or near this point, the density driving force for phase separation may not overcome surface tension forces, and a situation may arise in which part of the denser phase is trapped above the less dense phase, thus creating the appearance of a three-phase state. We believe that, in both of the systems that they studied, Davis and Morton³⁷ likely observed such a spurious three-phase state.

Table 1: Priority list for pairs of closest approach parameters ρ and σ to use in the asymmetric NRTL/eNRTL model. See Section 2.2 for discussion.

ρ	σ (m)
5	$5 \cdot 10^{-10}$
5	$1 \cdot 10^{-9}$
8.94	$1 \cdot 10^{-9}$
8.94	$5 \cdot 10^{-9}$
14.9	$5 \cdot 10^{-9}$
14.9	$1 \cdot 10^{-8}$
25	$1 \cdot 10^{-8}$
25	$5 \cdot 10^{-8}$

Table 2: Summary of ternary system examples.

Example No.	Figure No.	Ternary Type	System (1)/(2)/(3)	Temperature (K)
1	2, 3	1	[hmim][Tf ₂ N]/Ethanol/Water	295
2	4, 5	2	[HOhmim][Tf ₂ N]/1-Butanol/Water	295
3	6, 7, 8, 9	2a	[bmim][PF ₆]/Ethanol/Water	290, 298, 313
4	10, 11, 12, 13	3a/3b	[bmim][Tf ₂ N]/1-Butanol/Water	288

Table 3: NRTL binary interaction parameters (J/mol) estimated from binary data.

Example No.	Figure No.	Temp. (K)	Δg_{12}	Δg_{21}	Δg_{13}	Δg_{31}	Δg_{23}	Δg_{32}
1	2	295	-2222.5	4969.0	702.08	21820	-2568.6	6949.2
2	4	295	1948.7	1914.6	-5045.1	21276	-2566.9	12505
3	6	298	-4309.1	16476	-685.01	16672	-2556.2	6974.5
4	10	288	-3411.0	13019	-428.14	19105	-2555.4	12217

Table 4: UNIQUAC binary interaction parameters (J/mol) estimated from binary data.

Example No.	Figure No.	Temp. (K)	Δu_{12}	Δu_{21}	Δu_{13}	Δu_{31}	Δu_{23}	Δu_{32}
1	2, 3	295	2646.6	-743.47	4812.5	151.97	-245.79	1870.2
2	NA	295	1313.9	-113.41	3006.3	200.48	782.66	1471.3
4	11	288	67.986	1431.9	5811.7	1368.1	1959.4	2333.4

Table 5: eNRTL binary interaction parameters (J/mol) estimated from binary data.

Example No.	Figure No.	Temp. (K)	Δg_{12}	Δg_{21}	Δg_{13}	Δg_{31}	Δg_{23}	Δg_{32}
1	2	295	-8259.0	14230	-2707.1	21287	-2568.6	6949.2
2	NA	295	2169.0	2005.3	-2684.6	21072	-2566.9	12505
3	6	298	-7219.1	16431	-3992.3	17535	-2556.2	6974.5
4	12, 13	288	1152.2	800.05	-3636.3	20083	-2555.4	12217

Table 6: NRTL/eNRTL binary interaction parameters (J/mol) estimated from binary data.

Example No.	Figure No.	Temp. (K)	Δg_{12}	Δg_{21}	Δg_{13}	Δg_{31}	Δg_{23}	Δg_{32}
1	3	295	-2222.5	4969.0	167.62	11805	-2568.6	6949.2
2	5	295	1948.7	1914.6	-4440.3	16197	-2566.9	12505
3	7	298	-4309.1	16476	-223.68	10530	-2556.2	6974.5
3	8	290	-3879.9	16887	-110.02	10188	-2588.7	6908.2
3	9	313	-5060.2	15747	-1263.3	12015	-2493.4	7102.4
4	13	288	-3411.0	13019	133.55	8862.8	-2555.4	12217

Table 7: Solvent properties for eNRTL model.

Solvent	Temp.		$d(\text{g}/\text{cm}^3)$	ε	Reference
	(K)	M			
ethanol	290	46.07	0.78	24.4	Smyth and Stoops ³⁹
ethanol	295	46.07	0.78	23.7	Smyth and Stoops ³⁹
ethanol	298	46.07	0.78	23.2	Smyth and Stoops ³⁹
ethanol	313	46.07	0.76	21.0	Smyth and Stoops ³⁹
1-butanol	288	74.12	0.81	17.8	Smyth and Stoops ³⁹
water	288	18.02	1.00	82.1	Fernández et al. ⁴⁰
water	298	18.02	1.00	78.4	Fernández et al. ⁴⁰
water	295	18.02	1.00	79.6	Fernández et al. ⁴⁰
water	290	18.02	1.00	81.4	Fernández et al. ⁴⁰
water	313	18.02	0.99	73.4	Fernández et al. ⁴⁰

Table 8: Pure component size and shape parameters for UNIQUAC model.

Example No.	Figure No	Temp. (K)	UNIQUAC q reference	q_1	r_1	q_2	r_2	q_3	r_3
1	1	295	-CH ₂ -	11.62	12.51	1.97	2.11	1.40	0.92
2	3	295	-CH ₂ -	14.36	13.92	3.67	3.92	1.40	0.92
4	8	288	Water	7.29	11.20	2.62	3.92	1.00	0.92

List of Figures

Figure 1: Common ternary diagram types.⁵ The regions shaded in light and dark grey denote two-phase and three-phase envelopes respectively.

Figure 2: Ternary diagram (mol fraction) for [hmim][Tf₂N]/ethanol/water at 295 K (Example 1). Type 1 experimental data from Chapeaux et al.²³ All these symmetric-model predictions correctly predict a Type 1 system.

Figure 3: Ternary diagram (mol fraction) for [hmim][Tf₂N]/ethanol/water at 295 K (Example 1). Type 1 experimental data from Chapeaux et al.²³ and Type 1 predictions from the asymmetric NRTL/eNRTL model and the symmetric UNIQUAC model (best of symmetric models).

Figure 4: Ternary diagram (mol fraction) for [HOhmim][Tf₂N]/1-butanol/water at 295 K (Example 2). Type 2 experimental data from Chapeaux et al.²⁹ Symmetric NRTL model incorrectly predicts a three-phase region.

Figure 5: Ternary diagram (mol fraction) for [HOhmim][Tf₂N]/1-butanol/water at 295 K (Example 2). Type 2 experimental data from Chapeaux et al.²⁹ Asymmetric NRTL/eNRTL model correctly predicts Type 2 behavior.

Figure 6: Ternary diagram (mol fraction) for [bmim][PF₆]/ethanol/water at 298 K (Example 3). Type 2a experimental cloud point data from Najdanovic-Visak et al.³² Symmetric NRTL and eNRTL incorrectly predict Type 2 behavior.

Figure 7: Ternary diagram (mol fraction) for [bmim][PF₆]/ethanol/water at 298 K (Example 3). Type 2a experimental cloud point data from Najdanovic-Visak et al.³² Asymmetric NRTL/eNRTL model predicts Type 2a behavior on aqueous side of diagram.

Figure 8: Ternary diagram (mol fraction) for [bmim][PF₆]/ethanol/water at 290 K (Example 3). Type 2a experimental cloud point data from Najdanovic-Visak et al.³² Asymmetric NRTL/eNRTL model predicts Type 2a behavior on aqueous side of diagram.

Figure 9: Ternary diagram (mol fraction) for [bmim][PF₆]/ethanol/water at 313 K (Example 3). Type 2a experimental cloud point data from Najdanovic-Visak et al.³² Asymmetric NRTL/eNRTL model predicts Type 2a behavior.

Figure 10: Ternary diagram (mol fraction) for [bmim][Tf₂N]/1-butanol/water at 288 K (Example 4). Experimental cloud point data from Najdanovic-Visak et al.³⁶ is consistent with either Type 3a or Type 3b behavior, though Najdanovic-Visak et al.³⁶ proposed the Type 3b phase envelopes shown. However, recent experiments by Morton and Davis³⁷ imply, at least qualitatively, that this system is actually Type 3a (i.e., a two-phase region extends from the IL/water binary miscibility gap to the 1-butanol/water miscibility gap). Symmetric NRTL model incorrectly predicts Type 3 behavior, as indicated by the shaded three-phase region.

Figure 11: Ternary diagram (mol fraction) for [bmim][Tf₂N]/1-butanol/water at 288 K (Example 4). Experimental cloud point data from Najdanovic-Visak et al.³⁶ Symmetric UNIQUAC model incorrectly predicts Type 3 behavior, as indicated by the shaded three-phase region.

Figure 12: Ternary diagram (mol fraction) for [bmim][Tf₂N]/1-butanol/water at 288 K (Example 4). Experimental cloud point data from Najdanovic-Visak et al.³⁶ Symmetric eNRTL model predicts Type 3a behavior. See text for discussion.

Figure 13: Ternary diagram (mol fraction) for [bmim][Tf₂N]/1-butanol/water at 288 K (Example 4). Experimental cloud point data from Najdanovic-Visak et al.³⁶ The asymmetric NRTL/eNRTL model predicts Type 3a behavior. See text for discussion.

Figure B1: Ternary diagram (mol fraction) for [hmim][Tf₂N]/1-butanol/water, comparing experimental data sets of Chapeaux et al.²³ at 295 K and Davis and Morton³⁷ at 298 K.

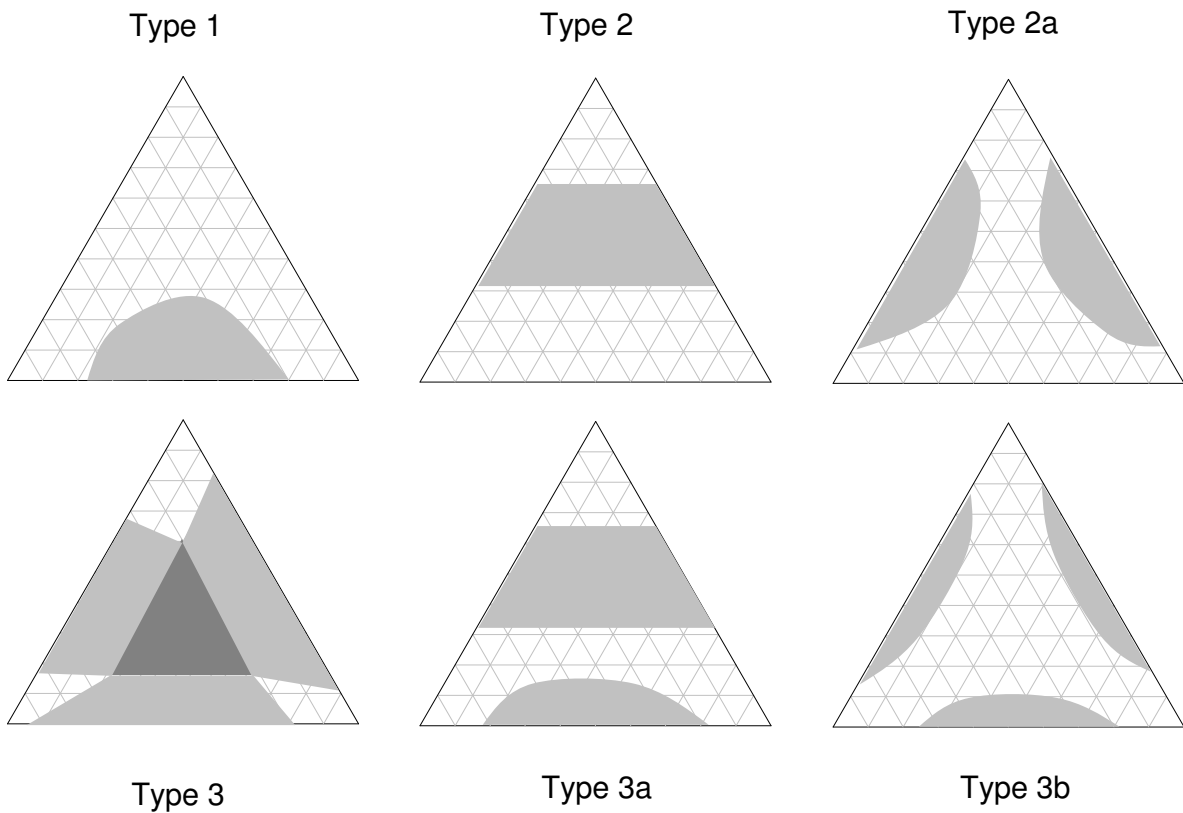


Figure 1: Common ternary diagram types.⁵ The regions shaded in light and dark grey denote two-phase and three-phase envelopes respectively.

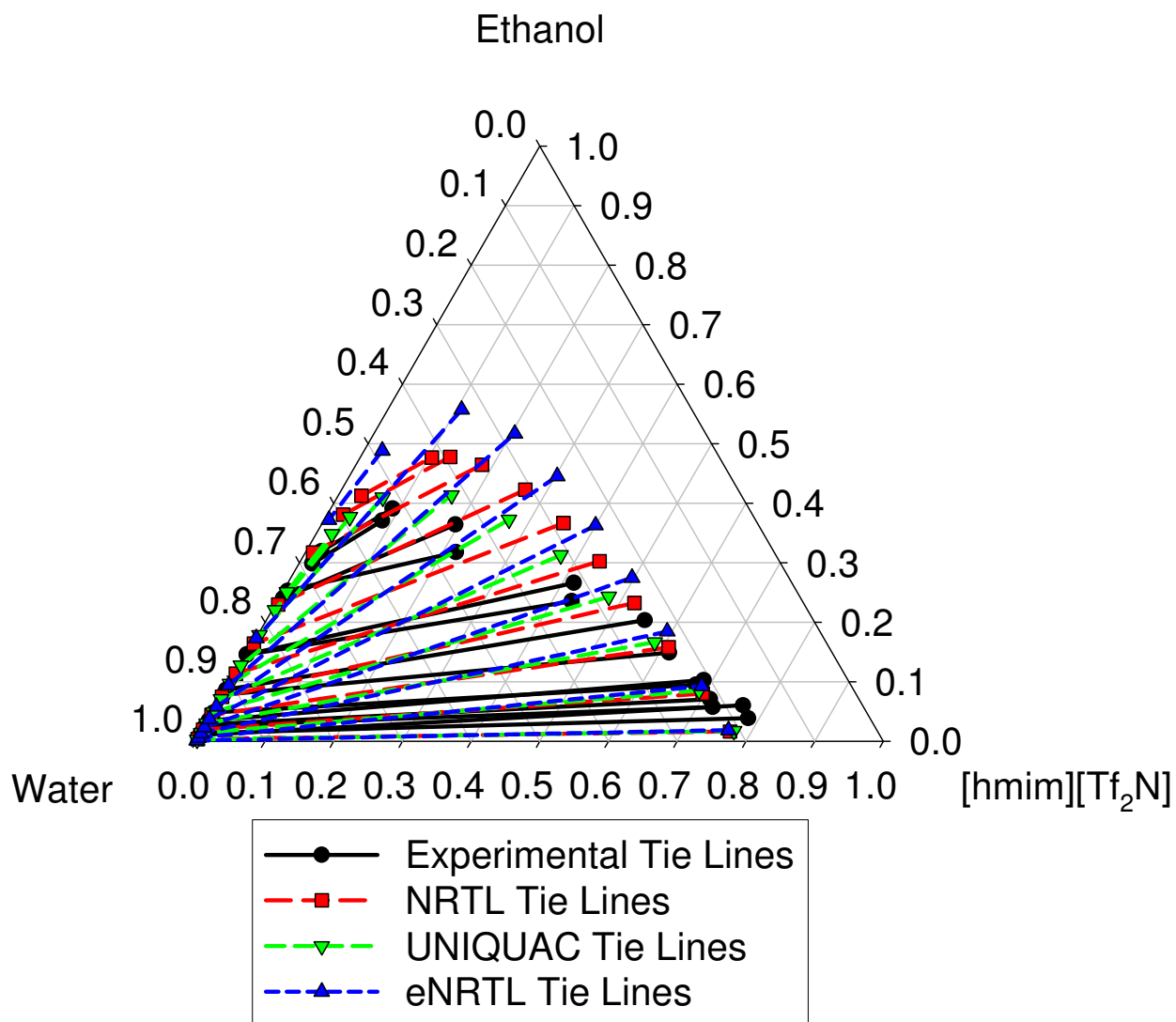


Figure 2: Ternary diagram (mol fraction) for [hmim][Tf₂N]/ethanol/water at 295 K (Example 1). Type 1 experimental data from Chapeaux et al.²³ All these symmetric-model predictions correctly predict a Type 1 system.

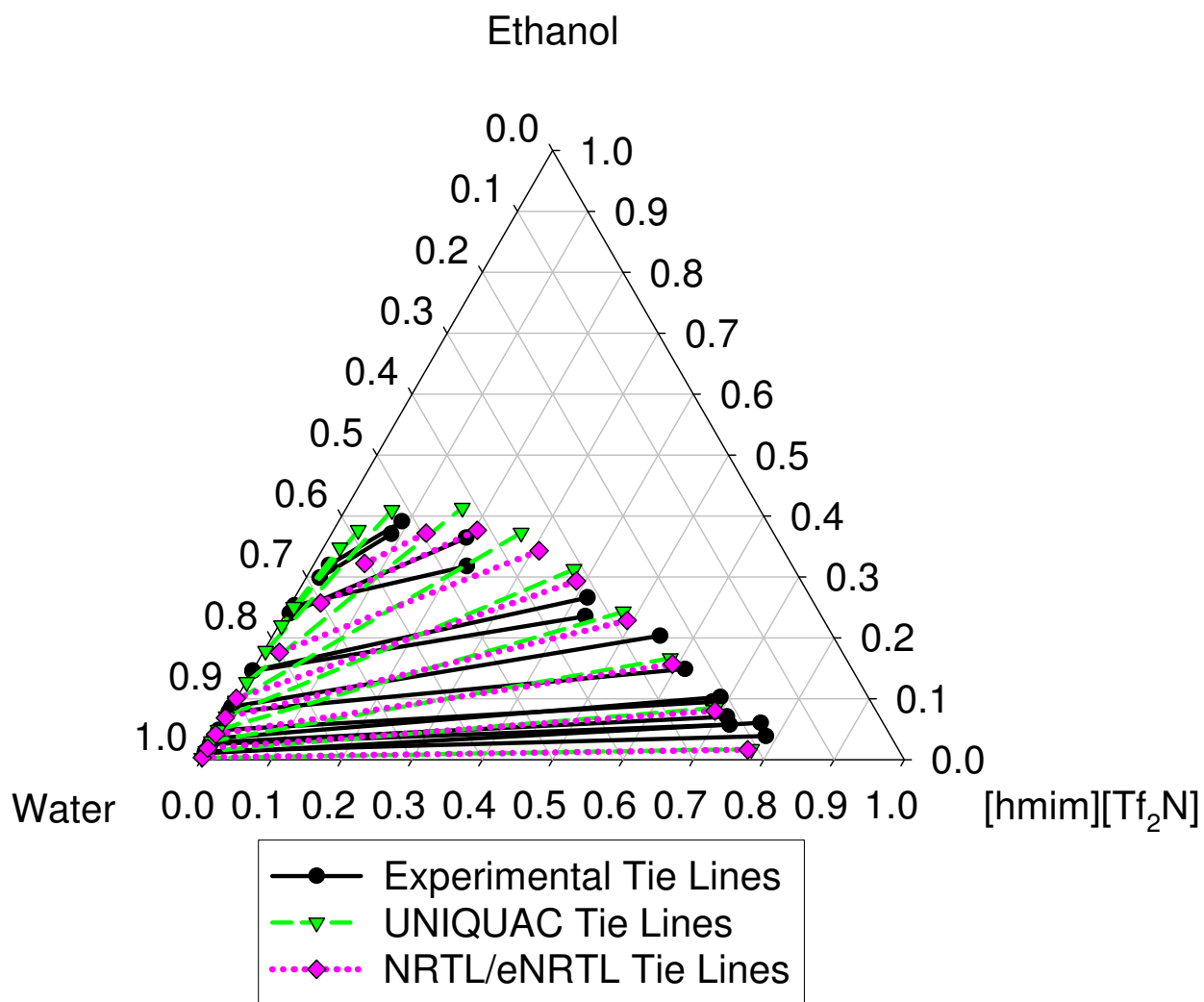


Figure 3: Ternary diagram (mol fraction) for [hmim][Tf₂N]/ethanol/water at 295 K (Example 1). Type 1 experimental data from Chapeaux et al.²³ and Type 1 predictions from the asymmetric NRTL/eNRTL model and the symmetric UNIQUAC model (best of symmetric models).

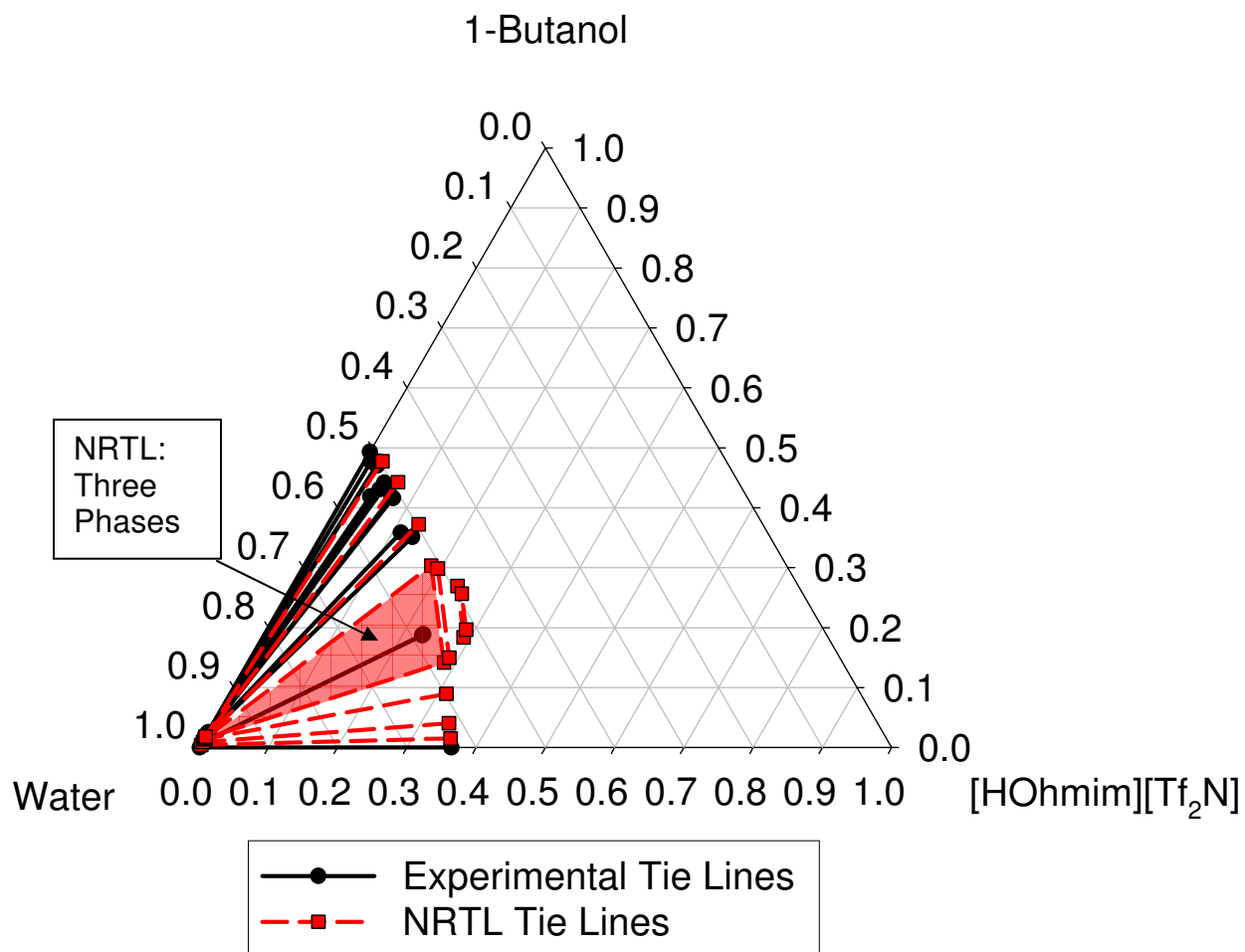


Figure 4: Ternary diagram (mol fraction) for [HOhmim][Tf₂N]/1-butanol/water at 295 K (Example 2). Type 2 experimental data from Chapeaux et al.²⁹ Symmetric NRTL model incorrectly predicts a three-phase region.

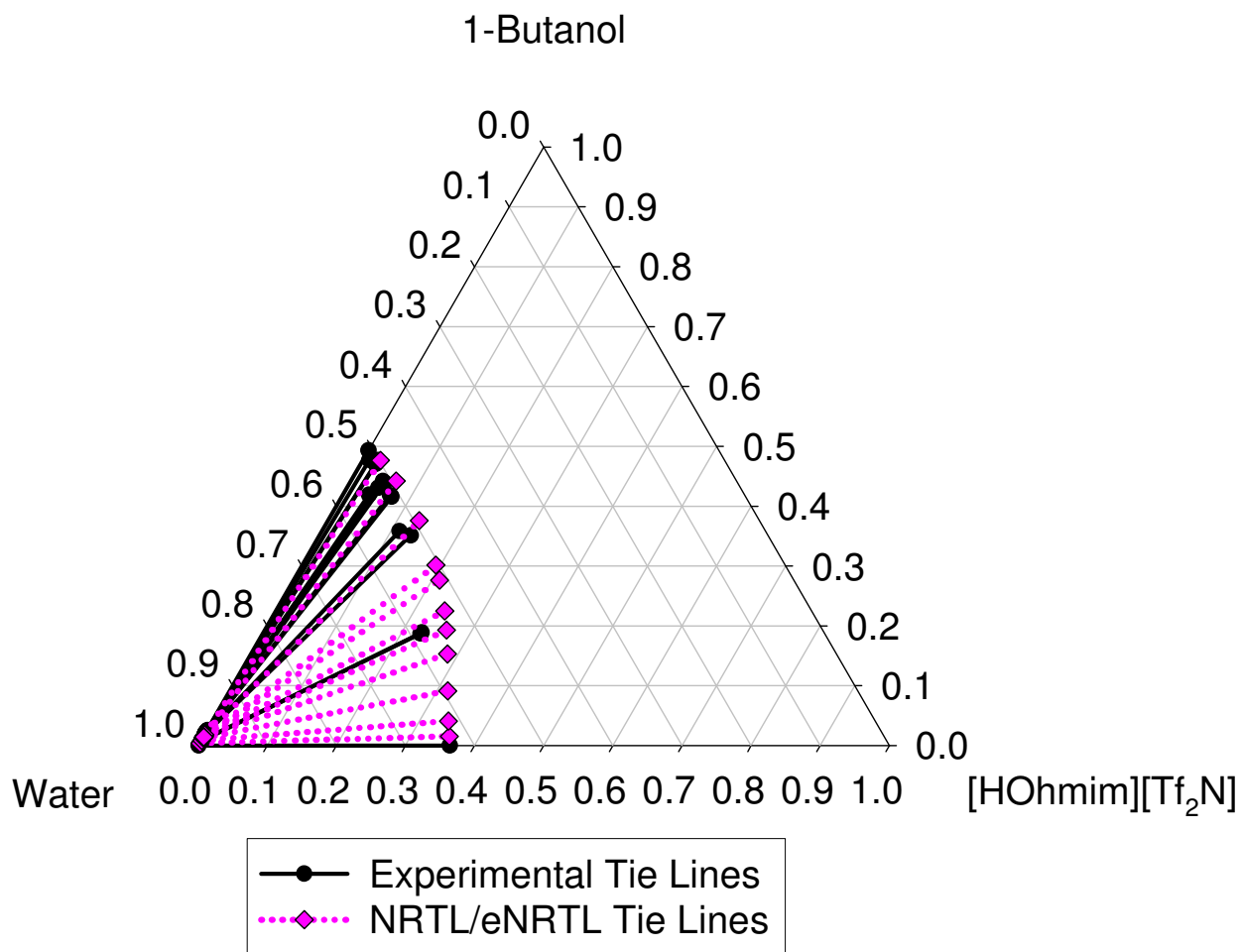


Figure 5: Ternary diagram (mol fraction) for [HOhmim][Tf₂N]/1-butanol/water at 295 K (Example 2). Type 2 experimental data from Chapeaux et al.²⁹ Asymmetric NRTL/eNRTL model correctly predicts Type 2 behavior.

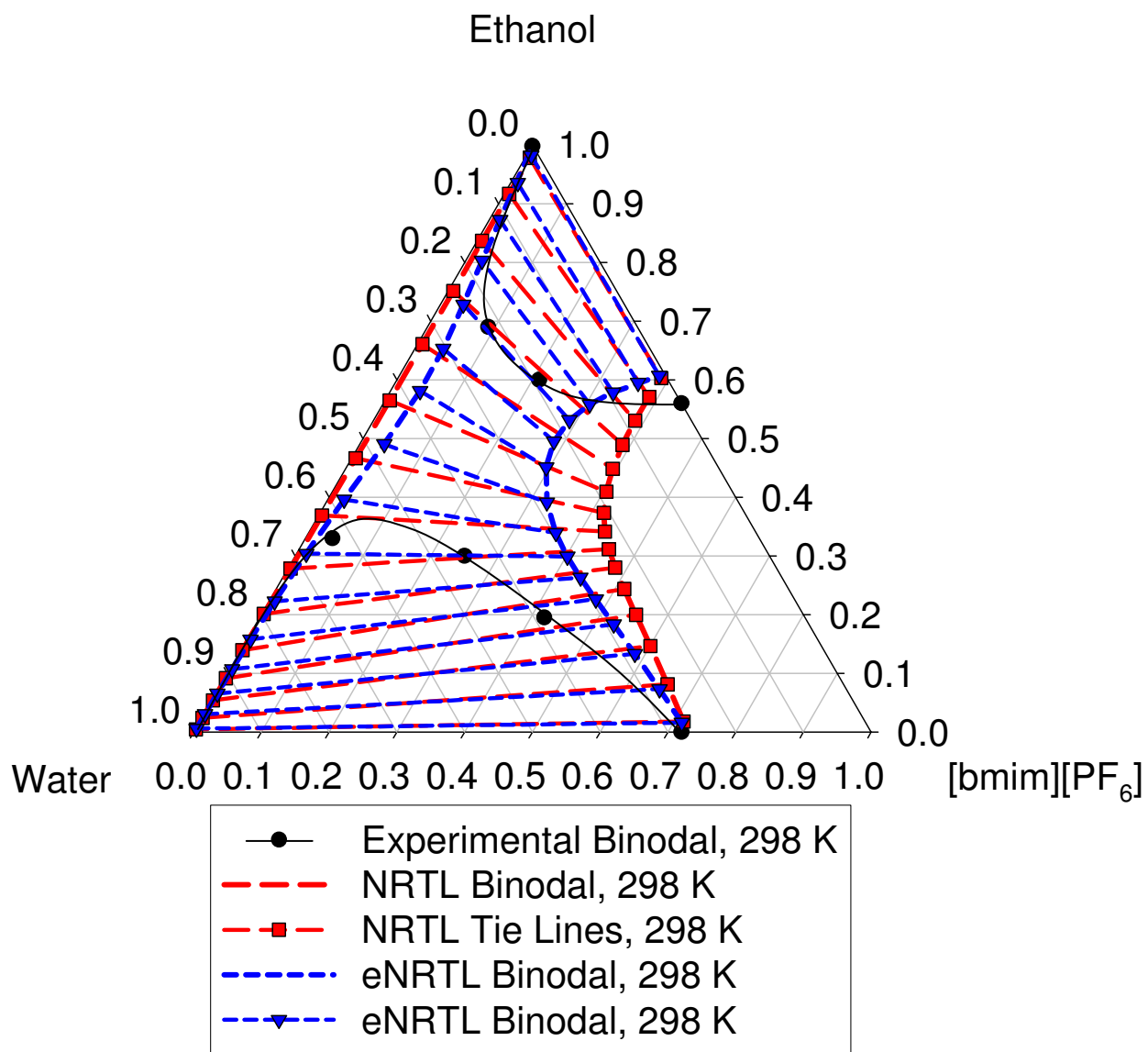


Figure 6: Ternary diagram (mol fraction) for [bmim][PF₆]/ethanol/water at 298 K (Example 3). Type 2a experimental cloud point data from Najdanovic-Visak et al.³² Symmetric NRTL and eNRTL incorrectly predict Type 2 behavior.

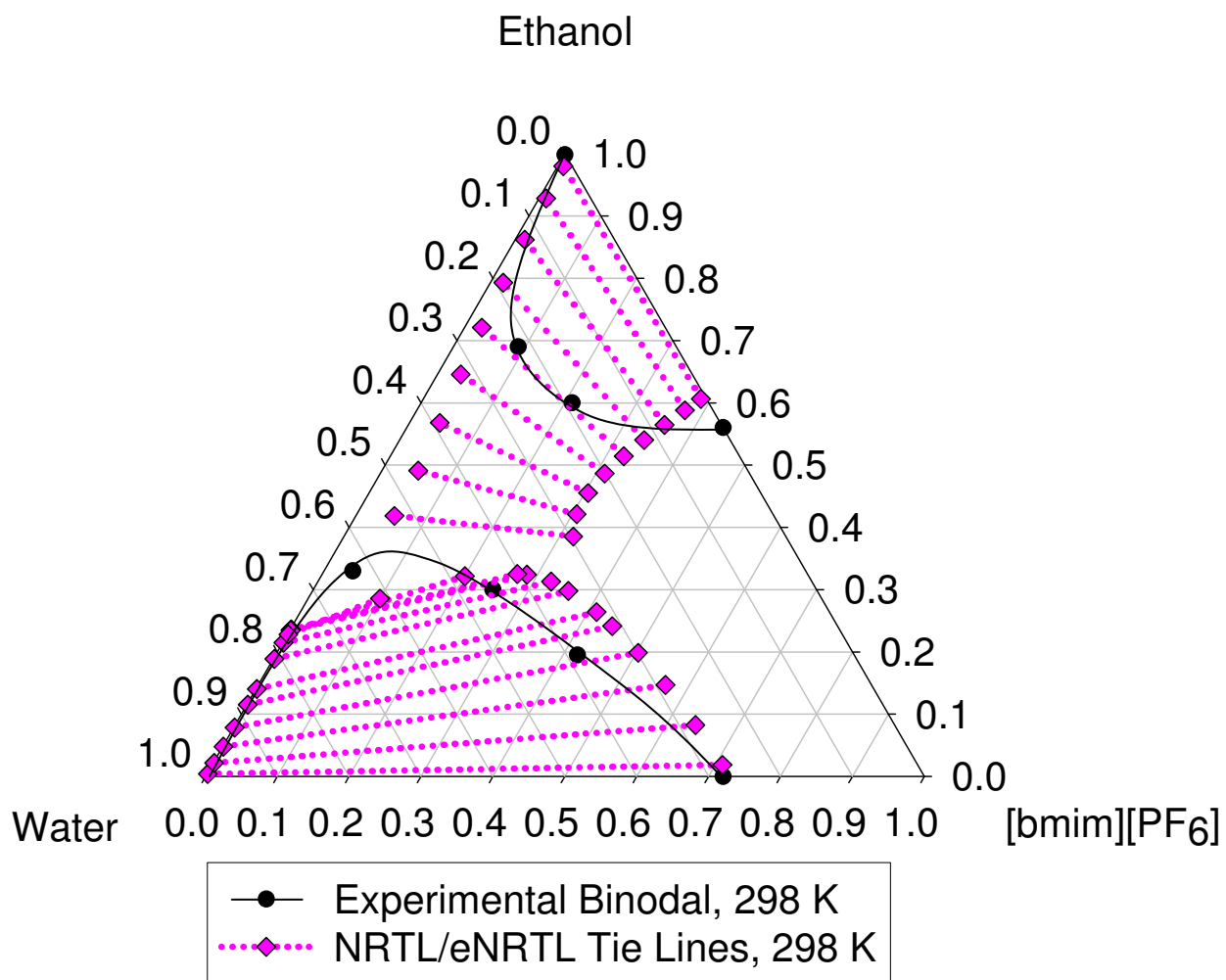


Figure 7: Ternary diagram (mol fraction) for [bmim][PF₆]/ethanol/water at 298 K (Example 3). Type 2a experimental cloud point data from Najdanovic-Visak et al.³² Asymmetric NRTL/eNRTL model predicts Type 2a behavior on aqueous side of diagram.

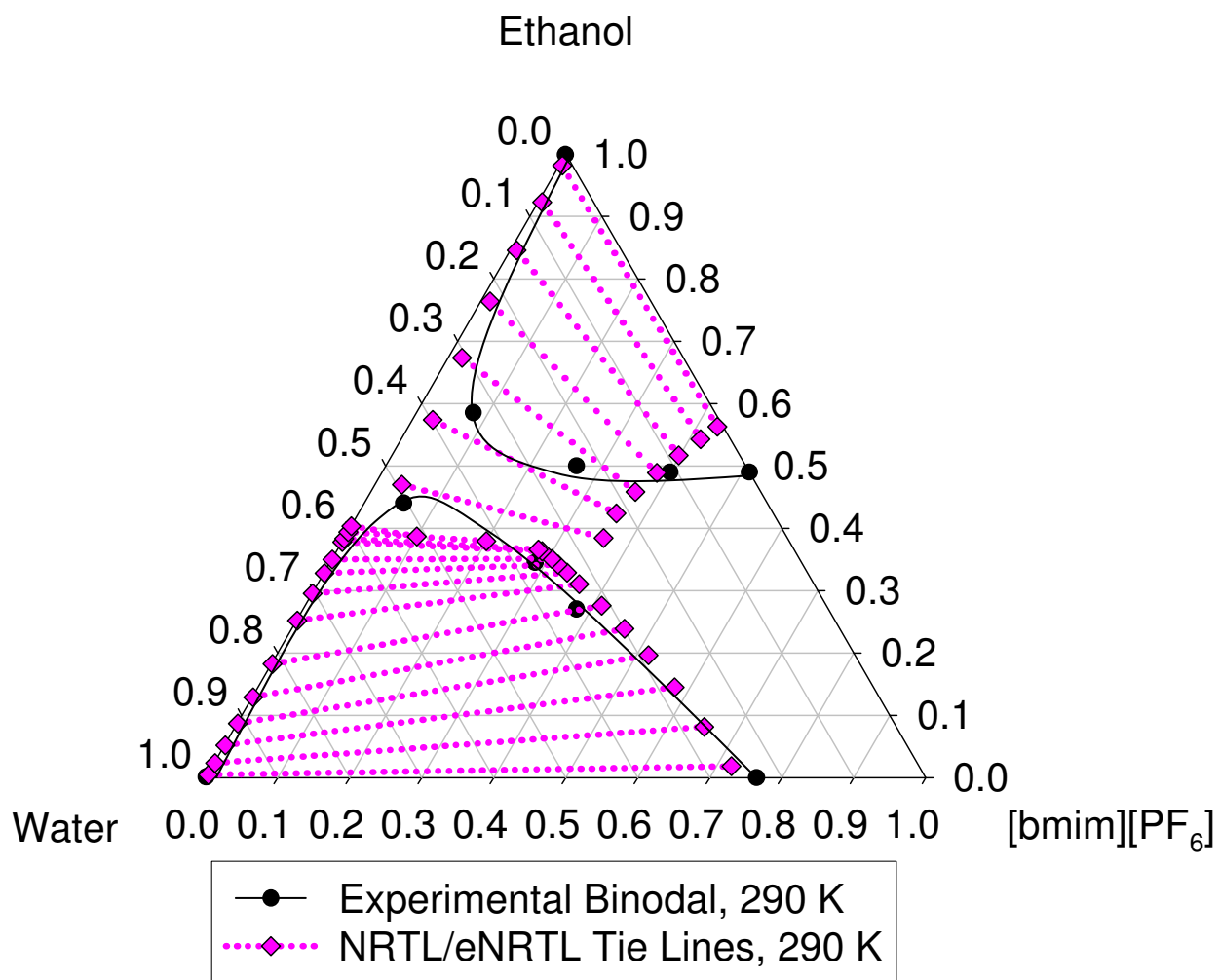


Figure 8: Ternary diagram (mol fraction) for [bmim][PF₆]/ethanol/water at 290 K (Example 3). Type 2a experimental cloud point data from Najdanovic-Visak et al.³² Asymmetric NRTL/eNRTL model predicts Type 2a behavior on aqueous side of diagram.

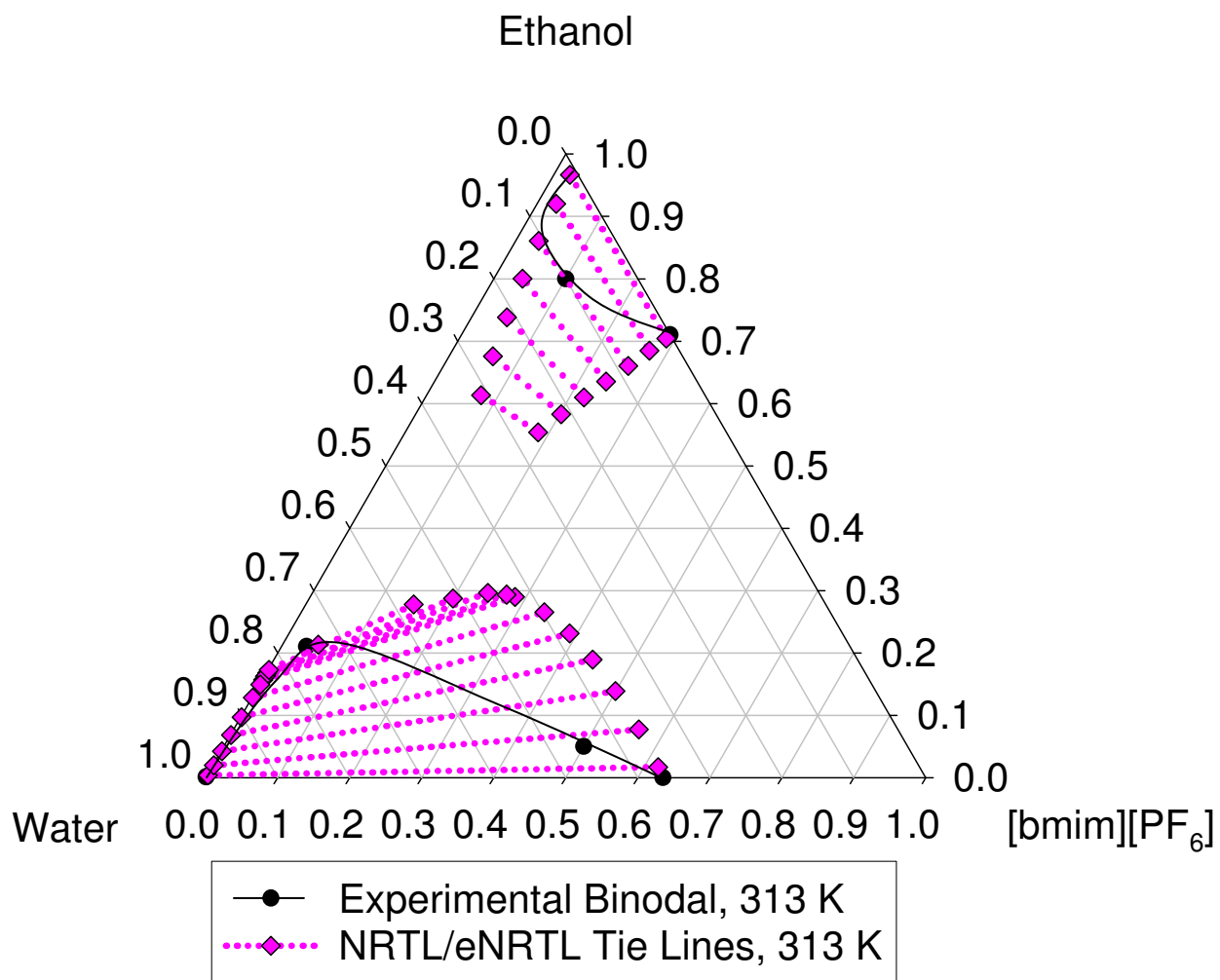


Figure 9: Ternary diagram (mol fraction) for [bmim][PF₆]/ethanol/water at 313 K (Example 3). Type 2a experimental cloud point data from Najdanovic-Visak et al.³² Asymmetric NRTL/eNRTL model predicts Type 2a behavior.

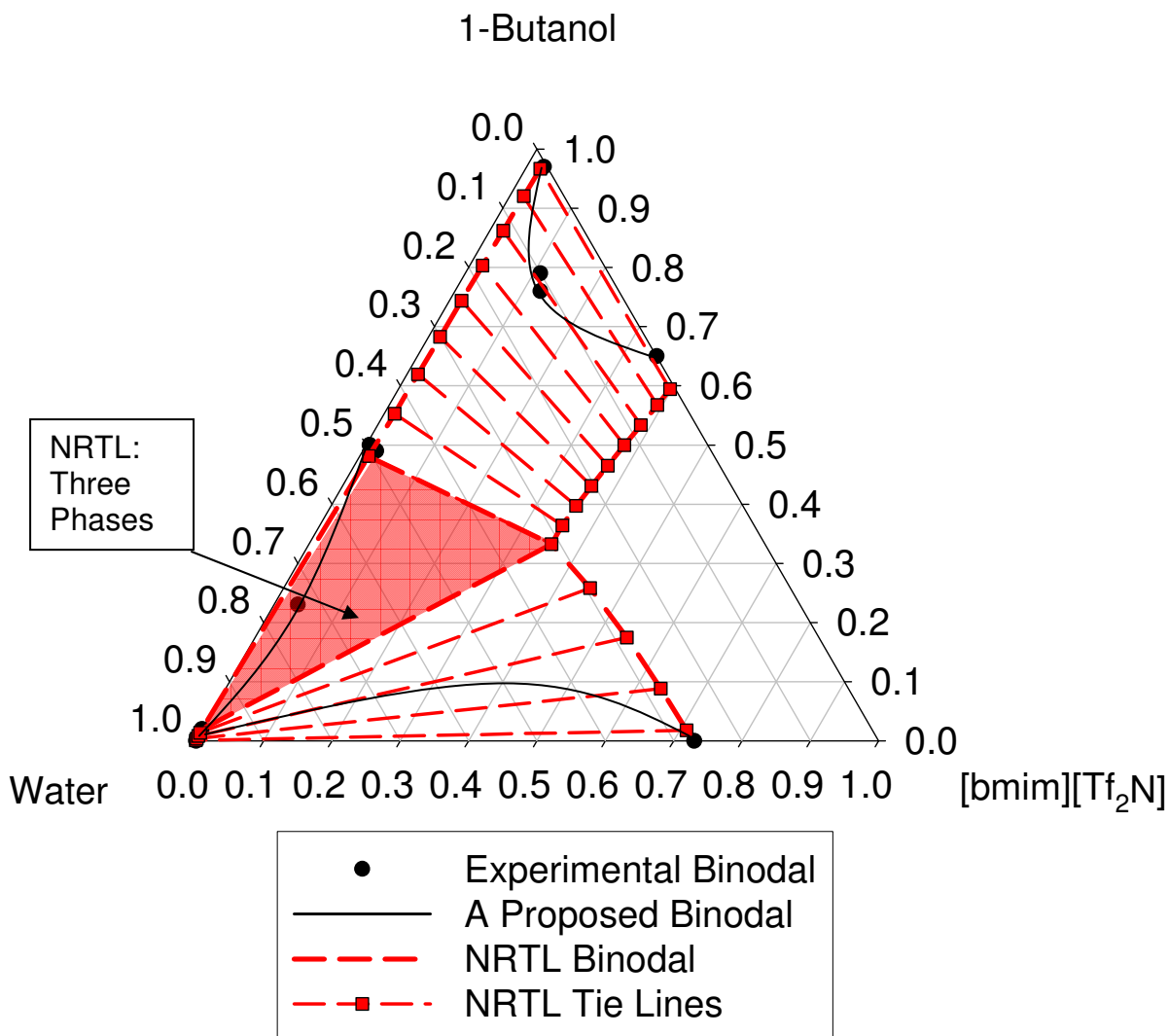


Figure 10: Ternary diagram (mol fraction) for [bmim][Tf₂N]/1-butanol/water at 288 K (Example 4). Experimental cloud point data from Najdanovic-Visak et al.³⁶ is consistent with either Type 3a or Type 3b behavior, though Najdanovic-Visak et al.³⁶ proposed the Type 3b phase envelopes shown. However, recent experiments by Morton and Davis³⁷ imply, at least qualitatively, that this system is actually Type 3a (i.e., a two-phase region extends from the IL/water binary miscibility gap to the 1-butanol/water miscibility gap). Symmetric NRTL model incorrectly predicts Type 3 behavior, as indicated by the shaded three-phase region.

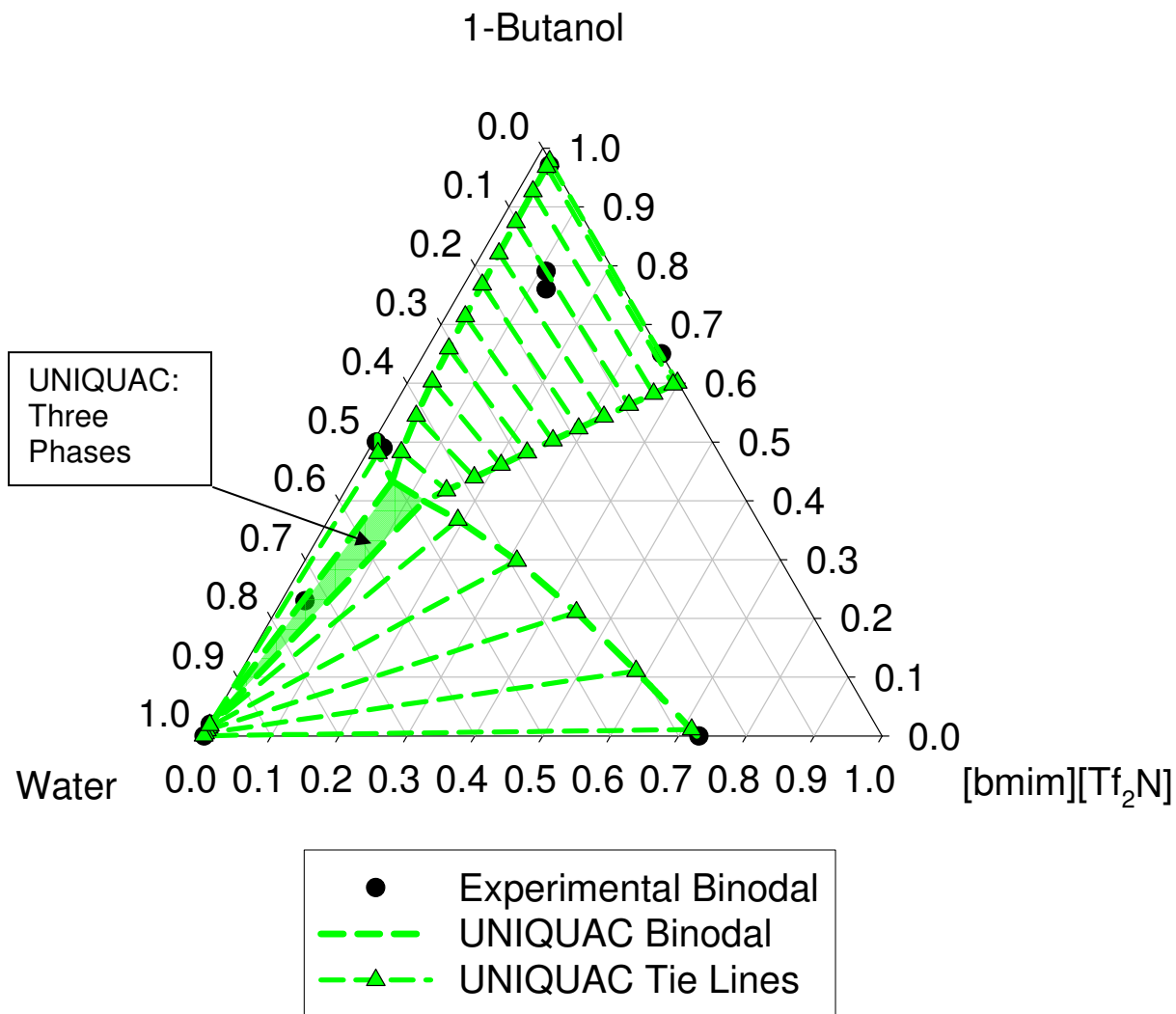


Figure 11: Ternary diagram (mol fraction) for [bmim][Tf₂N]/1-butanol/water at 288 K (Example 4). Experimental cloud point data from Najdanovic-Visak et al.³⁶ Symmetric UNIQUAC model incorrectly predicts Type 3 behavior, as indicated by the shaded three-phase region.

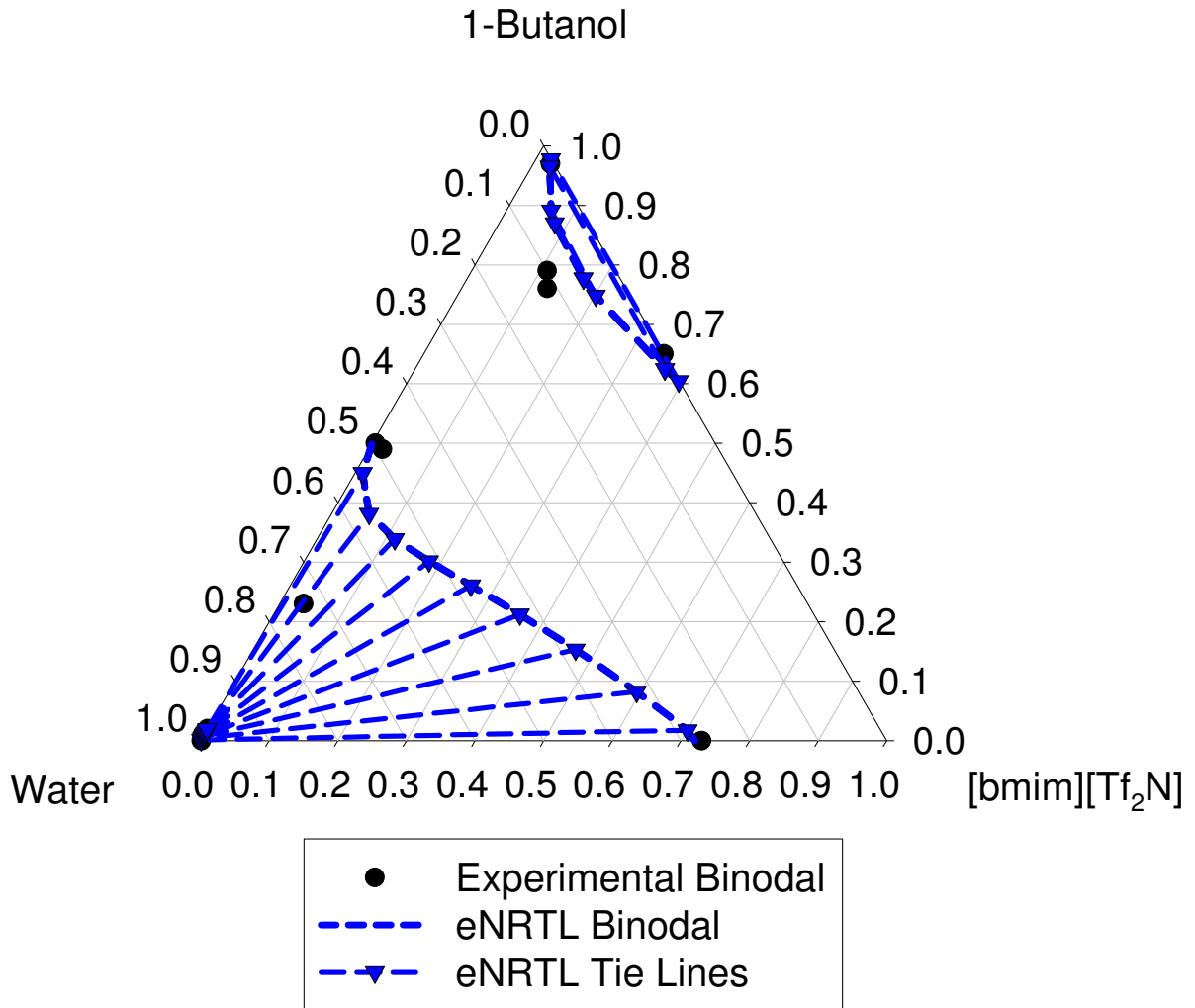


Figure 12: Ternary diagram (mol fraction) for [bmim][Tf₂N]/1-butanol/water at 288 K (Example 4). Experimental cloud point data from Najdanovic-Visak et al.³⁶ Symmetric eNRTL model predicts Type 3a behavior. See text for discussion.

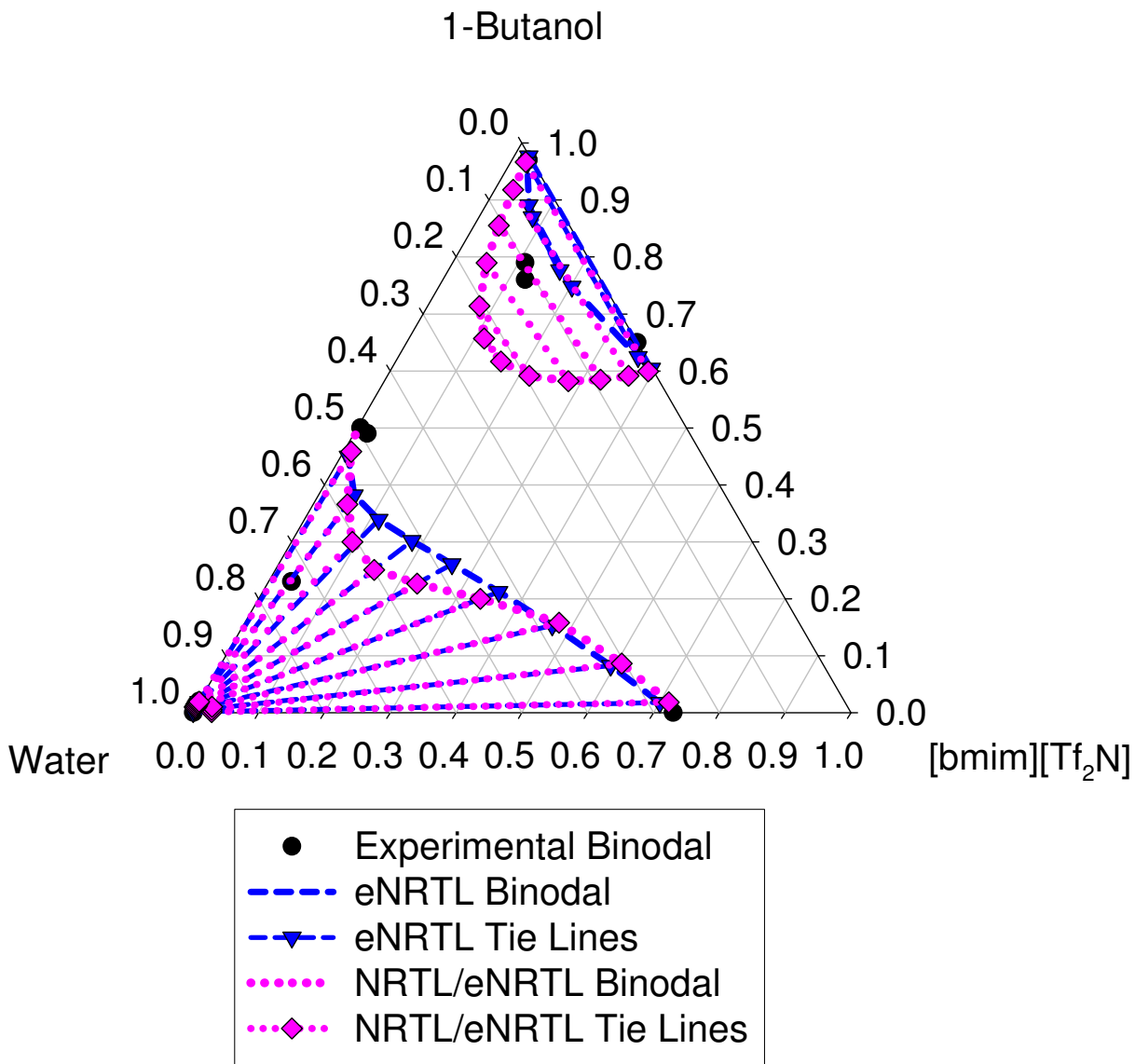


Figure 13: Ternary diagram (mol fraction) for [bmim][Tf₂N]/1-butanol/water at 288 K (Example 4). Experimental cloud point data from Najdanovic-Visak et al.³⁶ The asymmetric NRTL/eNRTL model predicts Type 3a behavior. See text for discussion.

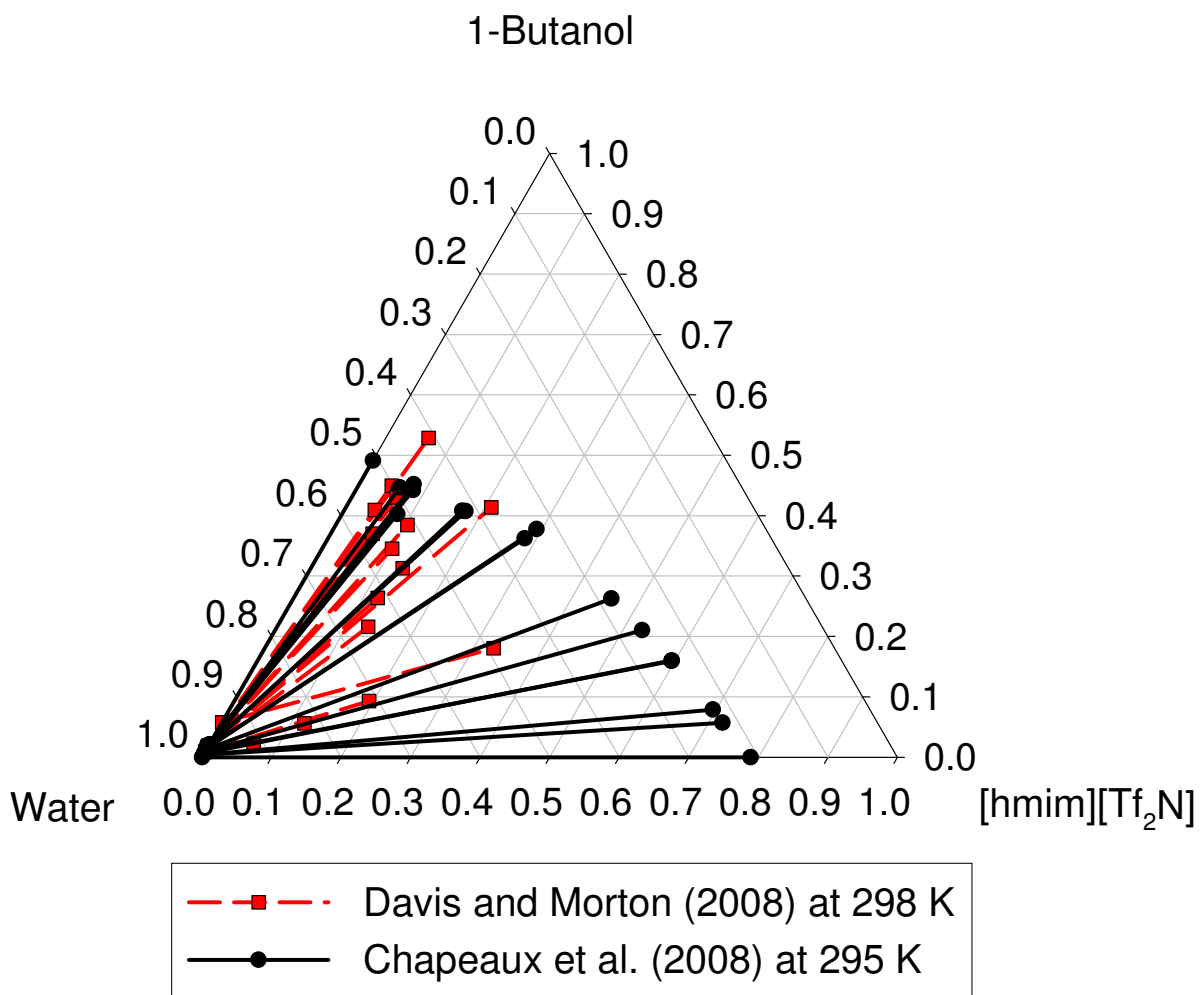


Figure B1: Ternary diagram (mol fraction) for [hmim][Tf₂N]/1-butanol/water, comparing experimental data sets of Chapeaux et al.²³ at 295 K and Davis and Morton³⁷ at 298 K.